Experimental investigation and modelling of a Solid Oxide Fuel Cell (SOFC) used in residential cogeneration applications

Étude expérimentale et modélisation d'une pile à combustible à oxyde solide (SOFC) utilisée dans les applications de cogénération résidentielle

Nicolas Paulus[1], Vincent Lemort[2]

[1] Department of Electromechanics, Industrial Engineering Higher Education Institution of the Province of Liège (HEPL), Liège, Belgium, nicolas.paulus@hepl.be
[2] Thermodynamics laboratory, University of Liège, Liège, Belgium, vincent.lemort@uliege.be

ABSTRACT. The much-needed energy transition brings special focus on fuel cell micro-combined Heat and Power (mCHP or micro-CHP) systems for residential uses, one of which is a Solid Oxide Fuel Cell (SOFC), fed by natural gas, designed to provide continuously 1.5 kW_{el} with an associated amazingly high expected Low heating Value (LHV) electrical efficiency of 60%. This power output can be modulated as desired down to 500 W_{el} and heat can also be recovered to partially contribute to the heat demand of the household. This system has been installed in a laboratory environment and has been specifically instrumented in order to evaluate its performance with different thermal loads and electrical output power settings. In this paper, focus is brought on the resulting thermal output and efficiencies, both thermal and electrical, which have also been modelled with great goodness of fit. With several electrical power outputs between the 500-1500 W_{el} range, this study shows total High Heating Value (HHV) total efficiencies up to 88-89% at minimal return temperatures (around 20°C) in the heat recovery circuit. Maximum LHV electrical efficiency has been found to be equal to 57% at nominal output power (regardless of the thermal loads), which is close to the manufacturer's target of 60%.
RÉSUMÉ. La transition énergétique met en lumière les systèmes de micro-cogénération à pile à combustible pour les usages résidentiels, dont un est une Pile à Combustible à Oxyde Solide, alimentée au gaz naturel, conçue pour fournir continuellement 1,5 kW_{el} avec une efficacité électrique exceptionnellement élevée attendue de 60% (pouvoir calorifique inférieur). Cette puissance de sortie peut être modulée à volonté jusqu'à 500 W_{el} et la chaleur peut également être récupérée pour contribuer partiellement à la demande de chauffage du ménage. Ce système a été installé au laboratoire et a été spécifiquement instrumenté afin d'évaluer ses performances thermiques à différents régimes de puissance électrique. Dans cet article, l'accent est mis sur le rendement thermique résultant et les efficacités, tant thermiques qu'électriques, qui ont également été modélisées. Avec plusieurs sorties de puissance électrique entre 500 et 1500 W_{el}, cette étude montre des efficacités totales (pouvoir calorifique supérieur) jusqu'à 88-89% à des températures de retour minimales (autour de 20°C) du circuit de récupération de chaleur. L'efficacité électrique maximale obtenue est égale à 57% (pouvoir calorique inférieur) à puissance nominale, ce qui est proche de l'objectif de 60% du fabricant.
KEYWORDS. experimental, fuel cell, energy analysis, efficiency, model, part-load, cogeneration, SOFC.
MOTS-CLÉS. expérimental, pile à combustible, analyse énergétique, efficacité énergétique, modélisation, charge partielle, cogénération, SOFC.

1. Introduction

The Intergovernmental Panel on Climate Change (IPCC) has recently reported a maximum carbon budget of 890 $GtCO_2$ that humanity can emit from January 1st 2020 in order for global warming to likely remain under the +2°C acknowledged limit compared to preindustrial levels [1].

This carbon budget necessitates an immediate and significant reduction in the annual carbon footprint. For Western European regions or countries such as Wallonia and France, current estimates place these footprints at 15.0 tCO_{2eq}/year and 9.2 tCO_{2eq}/year respectively [2], while the individual net-zero 2050 carbon footprint is projected to approximate 1.0 tCO_{2eq}/year per capita [2]. This imperative for decarbonization therefore extends to residential levels, highlighting the increasing relevance of cleaner technologies. Among these, combined heat and power (CHP) fuel cell systems stand out [3–6]. Notably,

they offer the dual benefits of efficient energy generation and the absence of SO_2 or NOx emissions [7,8].

One system, already commercialized and tested in inhabited dwellings in field-test applications [9], is a Solid Oxide Fuel Cell (SOFC) fed by natural gas, designed to provide 1.5 kW_{el} of nominal output power with an amazingly high announced Low heating Value (LHV) electrical efficiency of 60%, along with a heat recovery of 0.6 kW_{th} representing a LHV thermal efficiency up to 25%. The output power can be modulated down remotely (by the manufacturer, upon the owner's request) as wanted in the 0.5 - 1.5 W_{el} range, affecting those announced efficiencies, but it is not advised to completely shut it down. Indeed, the thermal cycles that would be induced would imply too intense temperature gradients, which are known to contribute to degradation by opening micro-cracks and delaminations (failure mode for which materials fracture into layers) [10]. It is known that start-up and shut-down procedures require appropriate control to ensure fuel cell durability [11] and it is believed that in this case, this is the reason why start-up operations have been reported in the user manual to last up to 30 hours.

The purpose of this paper is to report the laboratory test campaigns that have been conducted in the facilities of the University of Liege on this SOFC system. This study aims to verify the electrical and thermal efficiencies announced at nominal output power, as well as to investigate how part-load operations affect them, which have not been extensively studied in literature with commercialized mCHP fuel cells. In addition, a wide range of operating temperatures for the heat recovery system of the SOFC have been tested and reported in this paper. The novelty of this work also lies in the performance models that have been computed from the experimental results and that can be easily integrated in building simulation tools. This work was initially presented at the 36th International Conference on Efficiency, Cost, Optimization, Simulation and Environmental Impact of Energy Systems (ECOS 2023) [12] and selected for publication in this journal.

2. Description of the system and the test bench

Discarding its chimney, the system has approximately the same size as a dishwasher, as it can be seen in Figure 1. Its internal schematics has not been disclosed but has been discussed in a previous publication [9], based on observations of the system and cogeneration SOFC literature. Amongst other particularities, the reforming process of the inlet natural gas (into hydrogen) is not only internal, i.e. directly onto the stack, at the anode, but it also uses an external steam reformer upstream of the stack (called 'pre-former' [9]). It is worth mentioning that the hydrocarbons (partial or complete) internal utilization capability of the SOFC technology, which can consits in direct decomposition at the anode or direct electrochemical utilization [13], is in fact enabled thanks to its high operating temperatures [14]. This consitutes a major advantage compared to PEMFCs fed by hydrocarbons [15], i.e. the main other commercialized residential fuel cell technology, because it increases fuel flexibility, tolerance to contaminants and efficiency [13].

The test bench, presented in Figure 2, has been described in a previous publication [16]. It has been designed to control the heat recovery flow rate, through a variable speed circulator, and the operating temperatures, through a high-capacity cooling heat exchanger bypassed by a thermostatic three-way valve [16].

Figure 1. *Tested mCHP SOFC in ULiege laboratory facilities*

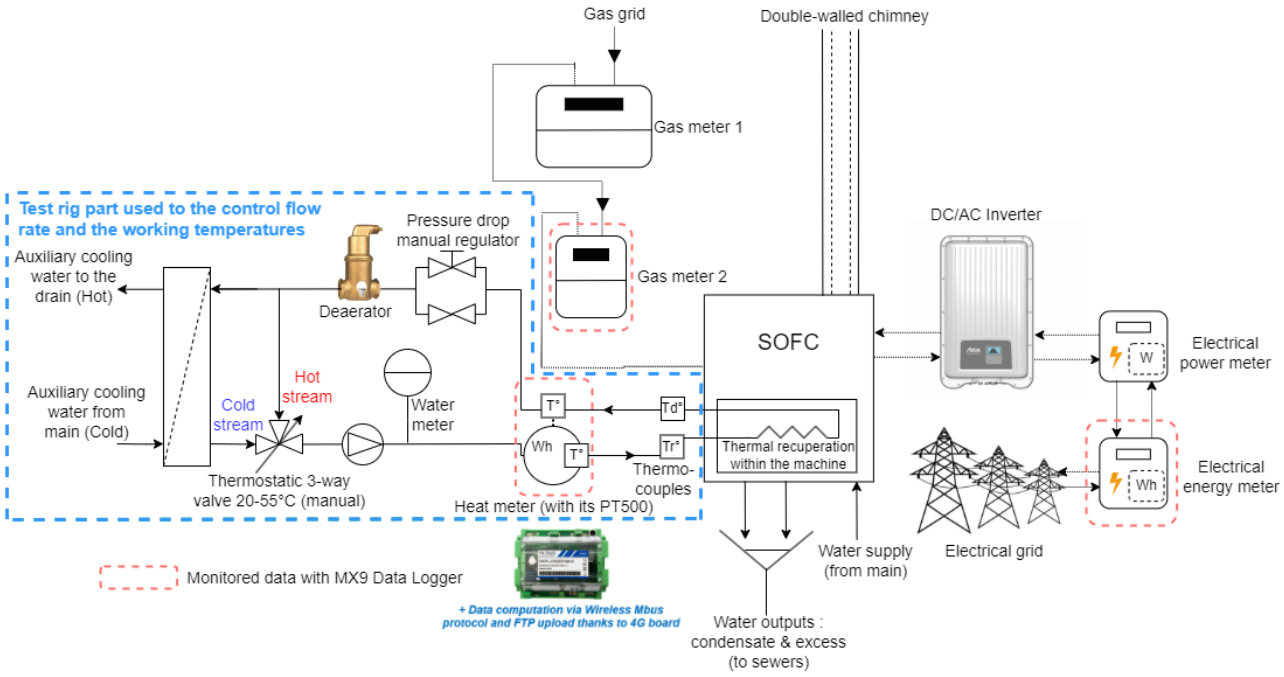

Figure 2. *Schematics of the SOFC test bench described in this paper*

2.1. *Measurement devices*

The test bench has also been designed to offer redundancy of the sensors required to compute electrical and thermal efficiencies: gas, electrical and heat meters (consisting of flow rate meters and temperature probes) have indeed all been doubled with field-test monitoring sensors connected to a Wireless M-bus (Meter-bus) data-logger [17]. It is worth mentioning that the same Wireless M-bus sensors have been implemented in a parallel field-test study on the same mCHP SOFC [9]. Therefore, the purpose of adding the same sensors as in the field-test study was to correlate the measurements and subsequently validate the field-test measurements. Main sensors used in the test bench for efficiency computation are shown in Figure 3 and Figure 4. Their references, accuracy and resolution have been reported in Table 1.

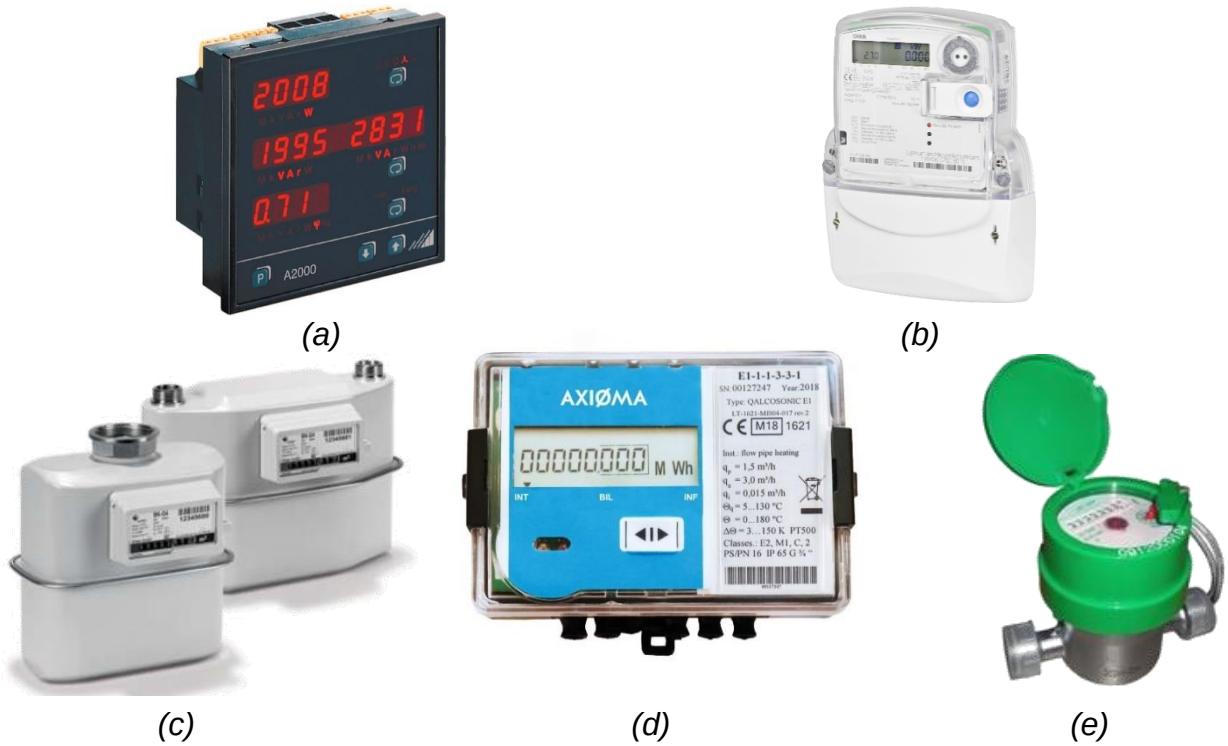

(a) *(b)* *(c)* *(d)* *(e)*

Figure 3. *Metering sensors used on the test bench: a) electrical power, electrical energy meter, c) gas meters, d) heat recovery meter (that computes supply and return temperatures as well as the flow rate)*

	Reference	Resolution	Accuracy
Recovery heat rate (and flow rate)	Qalcosonic E1 Qn2,5 qi=0.025m³/h | L=130mm	1 W_{th}* 1 L/h*	<5% Accuracy Class 2 [18]
Paired [19] depart and return temperature (PT500)* **	Qalcosonic E1 Qn2,5 qi=0.025m³/h | L=130mm	0,1 K*	<0,04 K at 293 K [20] <0,04 K at 333 K [20]
Recovery heat volumetric water meter* **	DHV1300	0.1 L	<2% (datasheet)
Paired [19] depart and return temperature* **	'type T' thermocouples	Analog signal	±1 K [21]
Electrical power	A2000	1 W_{el}	<0.5% (datasheet)
Electrical energy counter	Iskrameco MT174	10 Wh*	< 1% Accuracy Class 1 [22]
Gas volume counter	BK-G4T DN25 Qmax 6 m³/h	10 L*	<0.5% (datasheet)

** Data logger included ** Assumed from Class B* [20]*, highest tolerance figure for most common PT500 *** For redundancy of the heat rate calculation*

Table 1. *Specifications of the main sensors used to compute efficiency laboratory results*

The field-test electricity meter is a Iskraemeco MT174, shown in Figure 3(b). It computes two indexes of electrical energy (for production and consumption). Electrical power is not directly provided and must be established by taking the derivative of the energy index. The electrical power meter, which is shown in Figure 3(a), is an A2000 bidirectional electrical power meter that shows both the net electrical power consumed and generated.

It is important to mention that the generated power exported to the grid is reduced by the power consumed by the operation of the SOFC itself. In electrical production mode (which occurs for all the

test conducted in the laboratory), no electrical consumption is measured: the system provides for its own auxiliaries, except for the circulator of the (optional) heat recovery circuit, that is external to the SOFC and could be sized and chosen independently.

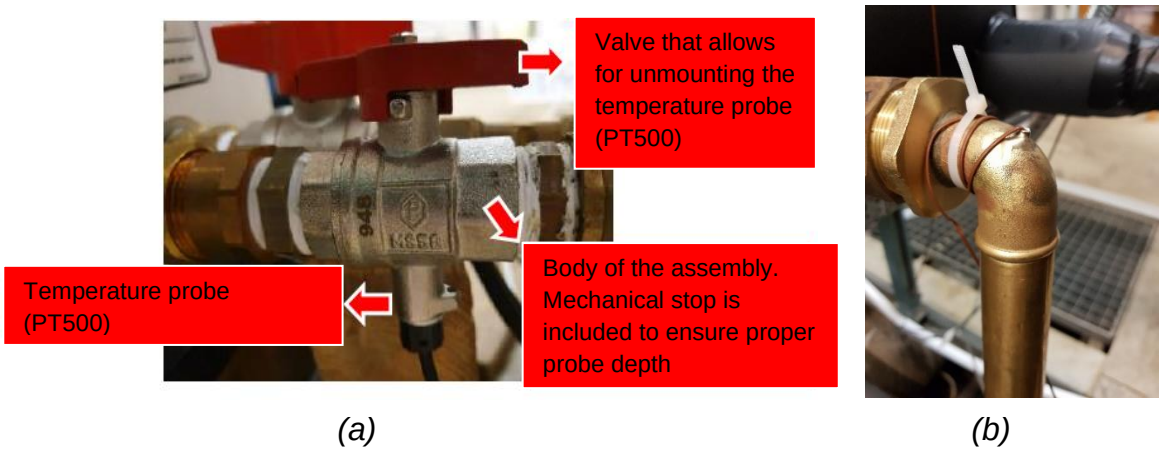

Figure 4. *Temperature measurements required to establish the heat recovery rate: a) separate PT-500 probe assembly required for the Qualcosonic E1 heat meter, b) thermocouple elbow immersion sleeve associated with the DHV1300 water meter*

The field-test heat meter sensor is a Qalcosonic E1, shown in Figure 3(d). It is preferably placed on the return line (as close as possible to the heating appliance to reduce the impact of thermal losses). It is composed of flow rate ultrasonic sensor combined with two PT-500 temperature probes to implement power calculations according to the first thermodynamics principle. One of those probes is included in the main body part of the sensor (where the flow rate measurement occurs) whereas the other probe has to be mounted in separate valve body (to place on the depart line as close as possible to the heating appliance). A commented photograph of this separate temperature probe assembly is presented in Figure 4(a).

The Qalcosonic sensor also provides the flow rate and temperature it measures. It also computes an energy index (by integration of the power measurement).

The heat meter is correlated to a specific combination of independent water flow rate and temperature measurements. On the one hand, ‘type-T’ thermocouples are placed in specifically manufactured immersion sleeves, as shown in Figure 4(b). Those are located at the recovery circuit return and depart (close to the PT-500 probes of the Qualcosonic E1 heat meter). The thermocouples are insulated after installation to ensure that the collected data to avoid the influence of radiation or convection with other sources. On the other hand, the water flow rate of the heat recovering circuit is also measured thanks to a DHV 1300 water meter, shown in Figure 3(e). It computes the volume of water that is passing through the sensor (thanks to the displacement of a rotating piston). It provides 10 pulses every litre so a frequency meter can be implemented to generate an analog signal. A specific calibration process allows for converting its frequency signal into the desired flow rate measurement.

Both gas metering diaphragm sensors reported in the test bench are BKG4T (temperature compensation implemented). They are shown in Figure 3(c).

2.2. *Testing procedure*

As explained, one purpose of the laboratory test campaigns is to evaluate the heat recovery performance according to the electrical power output of the SOFC (set remotely by the manufacturer and measured in the test bench). The heat recovery performance is studied related to the working temperature levels (it suffices to only control and measure the return temperature) and related to the heat recovery flow rate (also controlled and measured).

It has been chosen to discretize the net electrical output range into three: nominal (maximum) power (1500 W_{el}), minimal power (500 W_{el}) and an intermediate power setting (1000 W_{el}).

The flow rate range is also discretized into three. The chosen discretized flow rates are about 230 L/h, about 160 L/h and about 90 L/h. They correspond to the three positions of the chosen manual variable-speed circulator ('Yonos Para 15/6' by Wilo) and therefore cover its whole operating range.

The minimal return temperature that could be obtained depends on the auxiliary heat exchanger efficiency (and the temperature of the water mains which it is supplied from). At the time of the test campaign (September 2021), it was not possible to go lower than about 18°C. Maximum temperature of the return line is obtained by bypassing the auxiliary heat exchanger completely and depends on the thermal losses of all the heat recovery circuit to the air of the room (that can be considered at a constant temperature and humidity). At the time of the test campaigns, it was difficult to obtain return temperature higher than 47°C (corresponding to about 50°C of depart/supply temperature), especially for low output power setting (and therefore low heat recovery capacity). Beyond those extremes, it was then chosen to conduct the tests with 8 additional intermediate temperature levels: each temperature step is about 3 or 4 K.

For each tested operating conditions, one has waited at least 15 minutes to ensure for the system to be considered at steady-state.

2.3. *Equivalent energy contained in the consumed gas*

It is worth mentioning that all the laboratory tests were conducted in three separate days over two weeks in September 2021, allowing the electrical power output to be changed in between.

Natural gas consumed on the test bench comes from the grid. Its HHV has been provided hourly by the gas provider and the daily average values have been reported in Table 2.

	AC electrical power output	**HHV (given by the gas provider)**	**LHV (assuming HHV/LHV ratio of 1.1085 [23])**
Test sequence 1	1500 W_{el}	11,5762 kWh/m³	10,4431 kWh/m³
Test sequence 2	1000 W_{el}	11,5885 kWh/m³	10,4542 kWh/m³
Test sequence 3	500 W_{el}	11,6133 kWh/m³	10,4766 kWh/m³

Table 2. *Average HHV and LHV figures on the day of the test sequence*

It must be stated that the HHV figures of Table 2 have been measured by the gas provider in reference conditions (1 atm and 0°C), which are different from the gas delivery conditions. Therefore, the metered gas volume must be corrected to be applied to those HHV or LHV figures, following the method described in a previous publication [24]. Since the atmospheric pressure was not measured at the laboratory facility, it has been computed considering an assumed pressure at sea level of 101325 Pa and an ambient temperature of 15°C (see reference [24] for explanatory details).

The uncertainty levels of the HHV-LHV figures of Table 2 have not been given by the gas provider. Therefore, since the laboratory facility is receiving type 'H' natural gas ('rich' gas, as opposed to 'lean' gas, called type 'L' gas), the uncertainty level of those heating values can be assumed equal to ±234 Wh/m³, i.e. the same uncertainty level considered in the already referenced field-test study [9] for the site that also receives type 'H' gas.

3. Results

It is worth mentioning that the measured output power fluctuated in a range of only ± 3 W_{el} around the power output setting set remotely by the manufacturer (i.e. ± 0.6% in the worst case), not affected by the working temperature of the heat recovery system (nor its flow rate). Similarly, the gas consumption was observed to be very stable according to the output power setting and therefore not to depend on neither the temperature nor the flow rate of the heat recovery system. Indeed, it was observed to vary at worst in the ± 0.5% range. Those fluctuating ranges are even in the same order as the accuracy of the corresponding sensors, as shown in Table 1. Therefore, it has been established that electrical efficiency (not considering the power consumption of the circulator of the heat recovery system) also only depends on the output power setting (and is not affected by the state of the heat recovery system). Since the state of the heat recovery system affects the temperature of the flue gases, which heat up the incoming air required for the fuel cell reaction through the double-walled chimney (Figure 2), it could have indeed been imagined that it might have affected the electrical efficiency of the stack. However, it is not the case and one can assume that the internal heat management of the system is robust enough so the state of the heat recovery circuit only impacts the thermal efficiency of the system.

Indeed, only the thermal efficiency has significantly varied in all the laboratory test campaigns. So, the system's thermal efficiency dependency related to working temperature and flow rate of the heat recovery circuit is presented in Figure 5, Figure 6 and Figure 7, according to the electrical power output setting (respectively 1500 W_{el}, 1000 W_{el} and 500 W_{el}).

It is clear that the flow rate, in the tested range, has no significant influence on thermal efficiency. On the contrary, the efficiency decrease according to increased working temperatures is always noticeable and quite linear. It even increases (exponentially) as the electrical output power setting is lowered. Indeed, over similar tested working temperature ranges (of about 30°C each time), at 1500 W_{el}, the decrease in thermal efficiency is about 26 percentage points; at 1000 W_{el}, it is about 28 percentage points and at 500 W_{el}, it is about 35 percentage points. This exponential trend can be explained by the exponential relation between thermal efficiency and electrical output power, observable in Figure 8, which highlights efficiency results according to the power output setting. It also compares directly the results gathered in this particular experimental study with the one previously published by the manufacturer [25] (all obtained at a return temperature of 30°C). It is worth mentioning that those previous results have been presented in 2011 and might be relevant for a previous version of the system.

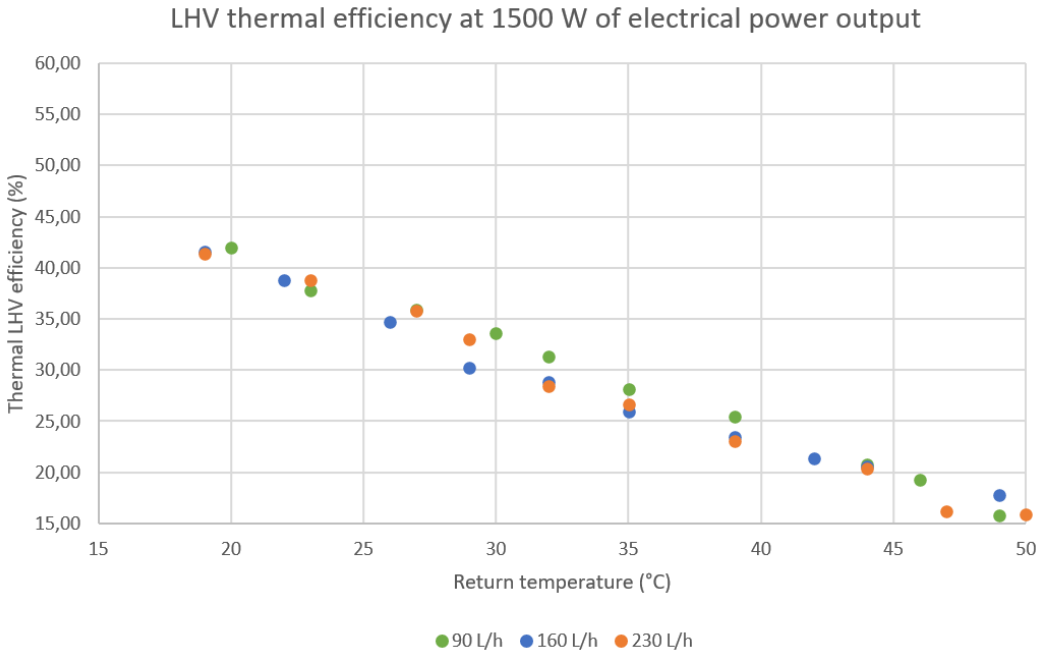

Figure 5. *LHV thermal efficiency of the SOFC related to working temperature (and water flow rate) at 1500 W_{el} of power output. LHV electrical efficiency has been found constant and equal to about 57%.*

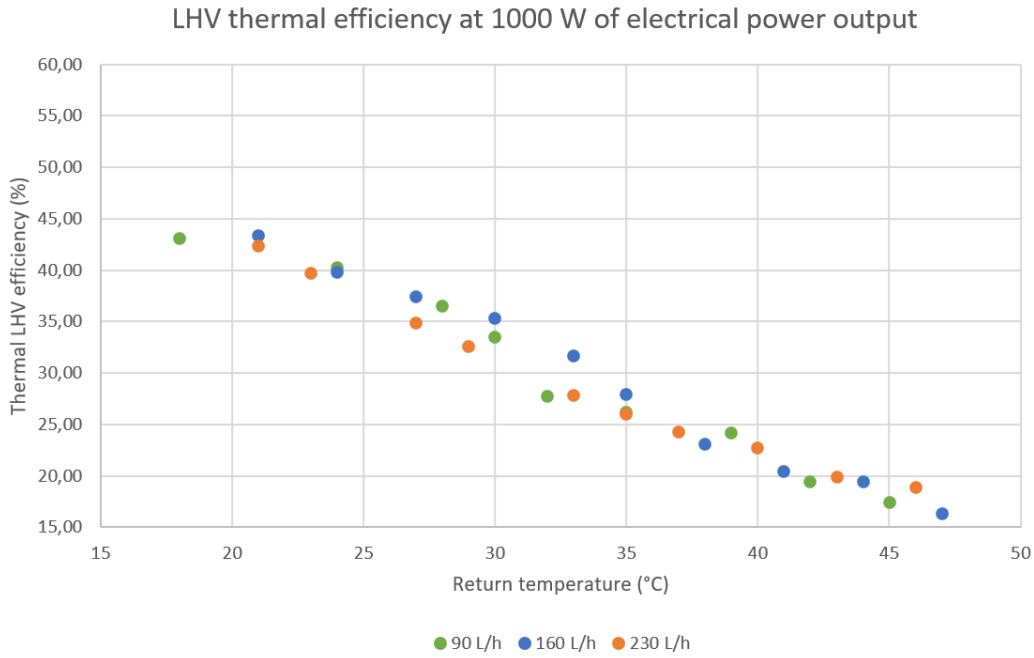

Figure 6. *LHV thermal efficiency of the SOFC related to working temperature (and water flow rate) at 1000 W_{el} of power output. LHV electrical efficiency has been found constant and equal to about 55%.*

As shown in Figure 8, total LHV efficiency is always about or above 80%. Figure 8 also shows that the laboratory efficiency variations between nominal electrical output power and 1000 W_{el} of output power is not significant. On the other hand, working at minimal power brings significant total efficiency decrease (explained by the 17 percentage points decrease in electrical efficiency, which is not balanced by the slightly higher thermal efficiency). It is quite trivial that partial load functioning leads to lower electrical and total efficiencies (mainly due to higher heat losses than at design operating conditions because the internal temperature must be kept constant [26]). Therefore, it is also quite normal that, as electrical efficiency increases, thermal efficiency decreases. This has been verified in literature for many CHP systems [27], as demonstrated with Figure 11, for which the experimental results of the BlueGen system reported in Figure 8 have been added for comparison.

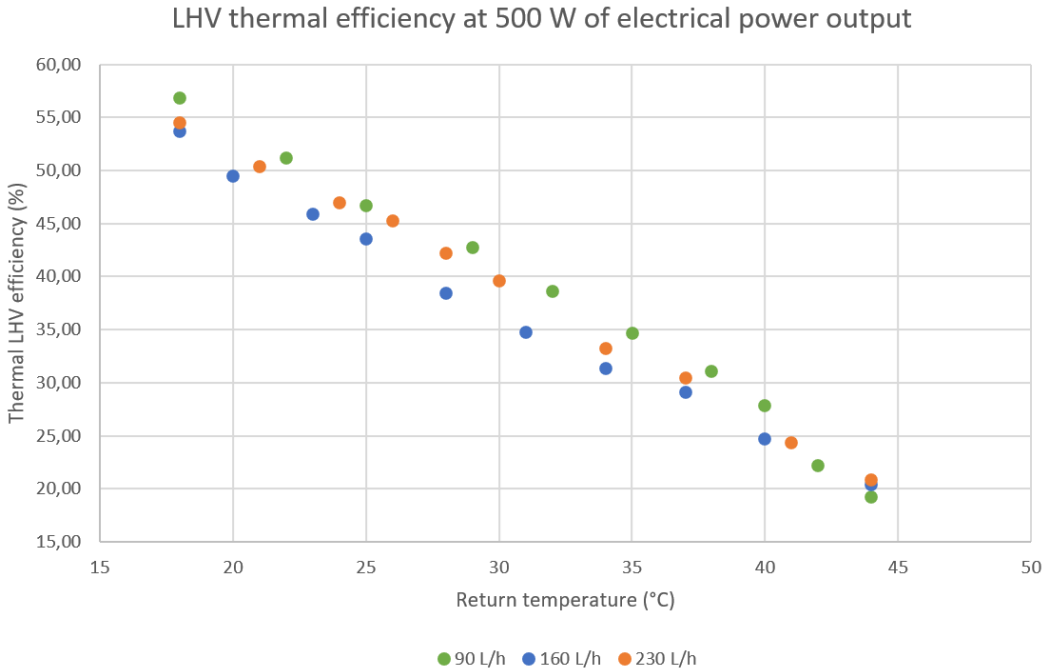

Figure 7. *LHV thermal efficiency of the SOFC related to working temperature (and water flow rate) at 500 W_{el} of power output. LHV electrical efficiency has been found constant and equal to about 40%.*

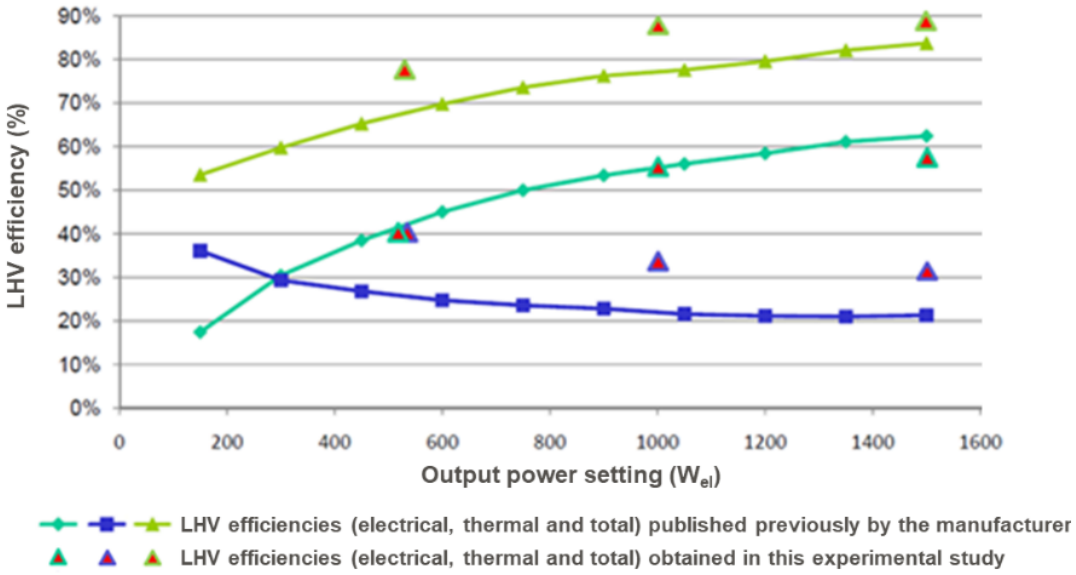

Figure 8. *LHV efficiency results obtained in this laboratory study superposed on reproduced ones previously published by the manufacturer [25] (all obtained with a return temperature of 30°C). System's version in the results published by the manufacturer has not been disclosed, neither as the way efficiencies have been measured or computed (which might explain the few differences).*

4. Performance models

Based on those results, the system has been modelled in two main steps with the Matlab software, starting with the thermal efficiency and finishing with the electrical efficiency.

As stated, the thermal efficiency of the system does not depend on the water flow rate of the heat recovery circuit. Therefore, the only influencing parameters for the thermal efficiency are the electrical output power $\dot{W}_{el}$ and the working temperature of the heat recovery circuit (which influence has been studied through its return temperature T_R). The resulting LHV thermal efficiency model (with its tremendous goodness of fit) is presented in Figure 9. It consists of a polynomial regression of the second order on both axes of all the results presented in Figure 5, Figure 6 and Figure 7, independently of the water flow rate of the heat recovery circuit. Between electrical power output $\dot{W}_{el}$ of 500 and 1500 W_{el}, this LHV thermal efficiency $\eta_{th,model}$ model is defined by Equation [1], whose parameters are provided in Table 3. Equation [1] has been nondimensionalized in Equation [2] :

$$\eta_{th,model}(\%) = f(\dot{W}_{el}, T_R) = p_{00} + p_{10}\dot{W}_{el} + p_{01}T_R + p_{20}\dot{W}_{el}^{\,2} + p_{11}\dot{W}_{el}T_R + p_{02}T_R^{\,2} \quad [1]$$

$$\eta_{th,model}(\%) = f(\lambda, T_R) = p_{00} + 1500p_{10}\lambda + p_{01}T_R + 1500^2p_{20}\lambda^2 + 1500p_{11}\lambda T_R + p_{02}T_R^{\,2} \quad [2]$$

Equation [2] is therefore expressed in terms of load factor λ, i.e. the nondimensionalized ratio between the electrical output power and the nominal power, equal to 1500 W_{el} in this case ($\lambda = \dot{W}_{el}/1500W_{el}$).

It must be stressed that this thermal efficiency model is valid on the tested heat recovery water flow rate. It is likely that higher heat recovery flow rate will not affect the model (because efficiency of the thermal exchange within the system seems to have reached its maximum asymptote). However, extremely low heat recovery flow rate will trivially reduce the efficiency of the exchange within the machine. It would therefore be considered as good practice to ensure at least 90 L/h of water flow rate in the recovery heat circuit (or to ensure that lower flow rates will not affect the thermal efficiency of this system). The model is likely to be valid in real applications since 90 L/h of water flow rate has been obtained at the 'lowest position' of the variable speed circulator used in the test bench (see Figure 2). Lower water flow rates could only occur with unlikely great pressure losses on the heat recovery circuit.

Thermal model parameters	Values
p_{00}	97.52
p_{10}	-0.03938
p_{01}	-1.699
p_{20}	9.855e-6
p_{11}	4.257e-4
p_{02}	3.249e-3

Table 3. *Parameters of the LHV thermal efficiency model of the SOFC of Equation [1] and Equation [2], valid between electrical power output $\dot{W}_{el}$ of 500 W_{el} and 1500 W_{el}*

It is worth mentioning that goodness of fit can indeed be studied easily with the Matlab software thanks to RMSE and R-square values. The following explanations have been provided by the Matlab Software support regarding those fitting variables [28]:

– R-square: This statistic measures how successful the fit is in explaining the variation of the data. Put another way, R-square is the square of the correlation between the response values and the predicted response values. R-square can take on any value between 0 and 1, with a value closer to 1 indicating that a greater proportion of variance is accounted for by the model;

– RMSE: This statistic is an estimate of the standard deviation of the random component in the data. RMSE value closer to 0 indicates a fit that is more useful for prediction.

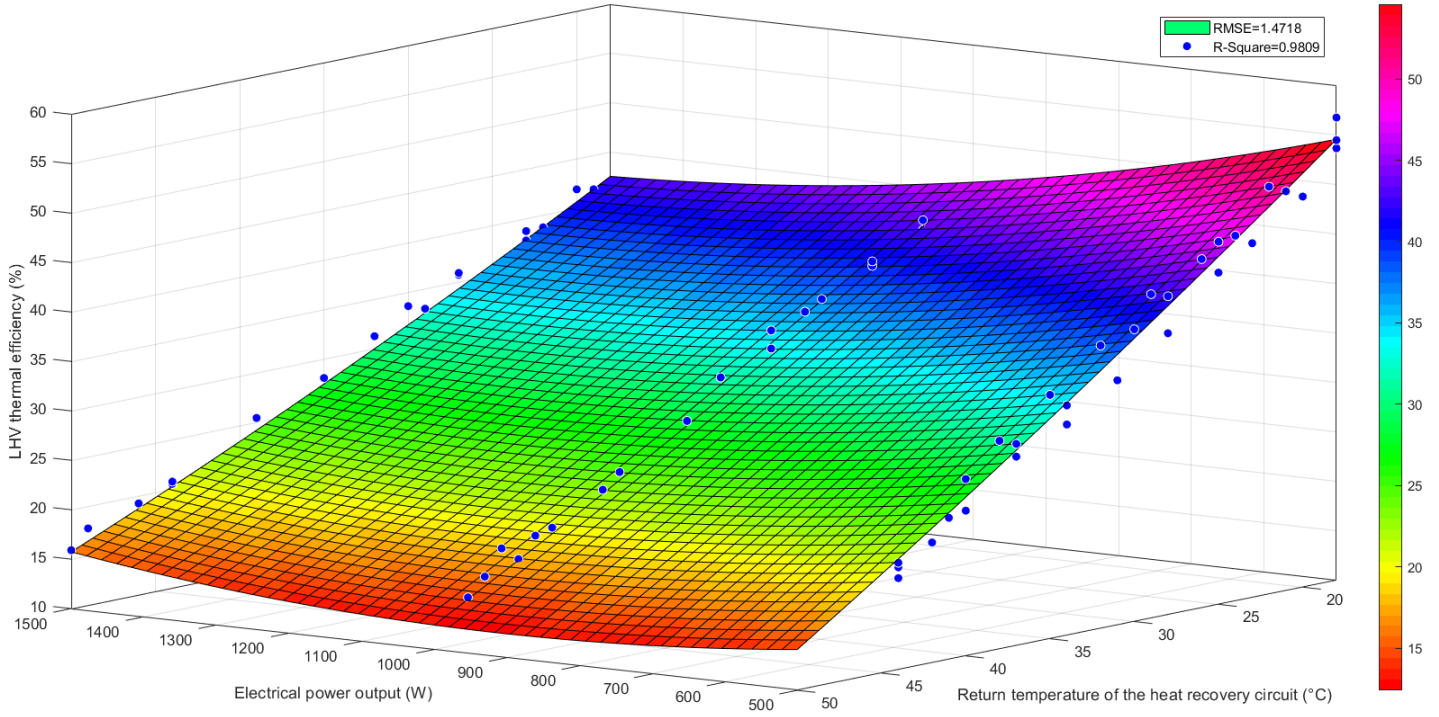

Figure 9. *Model of the laboratory BlueGen LHV thermal efficiency according to return temperature of the heat recovery circuit and electrical output power*

Modelling the LHV electrical efficiency is simpler as it does not depend on the return temperature of the heat recovery circuit (nor on its flow rate, as it was already the case with the thermal efficiency).

Again, the Matlab software has been used on all the results presented in Figure 5, Figure 6 and Figure 7. The resulting model is defined by the exponential Equation [3], which has been nondimensionalized in Equation [4] :

$$\eta_{el,model}(\%) = f(\dot{W}_{el}) = a \times \dot{W}_{el}^{\ b} + c \quad [3]$$

$$\eta_{el,model}(\%) = f(\lambda) = a \times 1500\lambda^{b} + c \quad [4]$$

Equation [4] is therefore expressed in terms of load factor λ, i.e. the ratio between the electrical output power and the nominal power, equal to 1500 Wel in this case ($\lambda = \dot{W}_{el}/1500\mathrm{W_{el}}$). Model parameters and goodness of fit indicators are given in Table 4.

Electrical model parameters and goodness of fit indicators	Values
a	-7.491e8
b	-2.82
c	57.64
RMSE	0.1687
R-Square	0.9996

Table 4. *Parameters and goodness of fit indicators of the LHV electrical efficiency model of the SOFC of Equation [3] and Equation [4]*

5. Discussion

5.1. *Comparison with previously published results*

LHV electrical efficiency at nominal power is about 3 percentage points behind the manufacturer target (one has obtained 57% experimentally and not 60% as stated in the Introduction) and this could be explained by the intrinsic statistical difference between production units and/or simply by the natural ageing of the stack (as shown in Figure 10). Indeed, the tested machine had already been operated for about 6000 hours at the times of the tests. At lower electrical power (1000 W_{el} and 500 W_{el}), the laboratory electrical efficiency results seem to be relevant with the 2011 results of Figure 8 [25]. On the other hand, it seems that heat recovery has been significantly improved since the earlier manufacturer's publication in 2011, probably achieved with the use of an internal recovery heat exchanger of larger size.

By deduction of Figure 5, the 25% LHV thermal efficiency announced by the manufacturer (as stated in the Introduction) is relevant with a return temperature of 40°C, which is sufficient in some DHW production applications as well as if the SOFC was directly connected to high-temperature terminal units (in older dwellings, for example). This SOFC mCHP performance has been compared with other well-known cogeneration technologies in Figure 11 [27]. It confirms that fuel cells (especially SOFC's) allow for achieving much higher electrical efficiencies than other technologies.

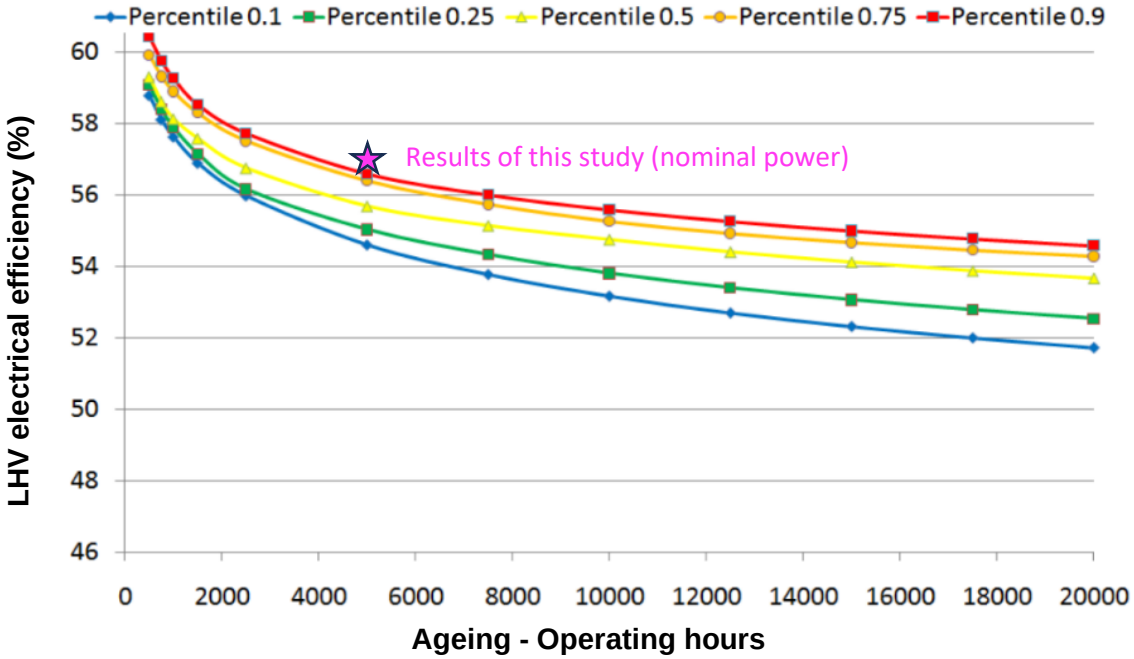

Figure 10. *Statistical analysis of production systems back in 2011 [25] expressed in terms of LHV electrical efficiency decay over time at nominal output power (1500 W_{el}). The version of the system in the results published by the manufacturer has not been disclosed. Reproduced from reference with the addition of the laboratory results obtained in this work.*

5.2. *External weather conditions*

At the time, it was decided not to monitor the external temperature and humidity during the test campaigns. Looking at the outcomes published in this paper, there are no unexpected results that are significant enough to be related to any weather variation that has occurred during the test campaigns. Therefore, with such a SOFC system, with tremendously high internal temperatures around 800°C [29], it could be considered that moderate external temperature and humidity variations (typical of Western Europe's climate) have no significant influence on the efficiencies of the system. It is worth mentioning that there were also neither any significant influence of external weather conditions that could have been inferred from the field-test study previously published about that particular SOFC system [9].

The efficiencies reported in Figure 11 are put in perspective with a line (lower dotted one) representing the reference conventional power that the micro-CHPs must beat (i.e. the average grid efficiency for electrical generation and the gas condensing boiler for heat production). Average efficiency of the grid electrical mix is considered to be at 40 % HHV (as comparison, the one of UK in 2013 was about 38.6% LHV, i.e. 34.8% HHV [30]). Reference thermal efficiency of condensing gas boiler is considered to be at 90% HHV (as comparison, yearly HHV efficiency figure of field-tested gas condensing boiler have been reported in the 82-89% range [31] whereas the Walloon energy regulator in Belgium has stated, based upon field-test studies, that reference state-of-the-art gas condensing boilers have efficiencies of 90% LHV, i.e. 81.2 % HHV [32]). The maximum physically possible upper limit considered in Figure 11, corresponding to total HHV efficiency of 100%, is represented by the upper dotted line. The experimental results of this SOFC system at 30°C of return temperature, reported in Figure 8 according to the output power setting, have been added to Figure 11 considering a 1.1085 HHV to LHV ratio [23]. Still in Figure 11, the efficiency results over the upper line (total efficiency results over 100% HHV) are most likely due to measurement uncertainty, especially regarding how the HHV is accounted for [24].

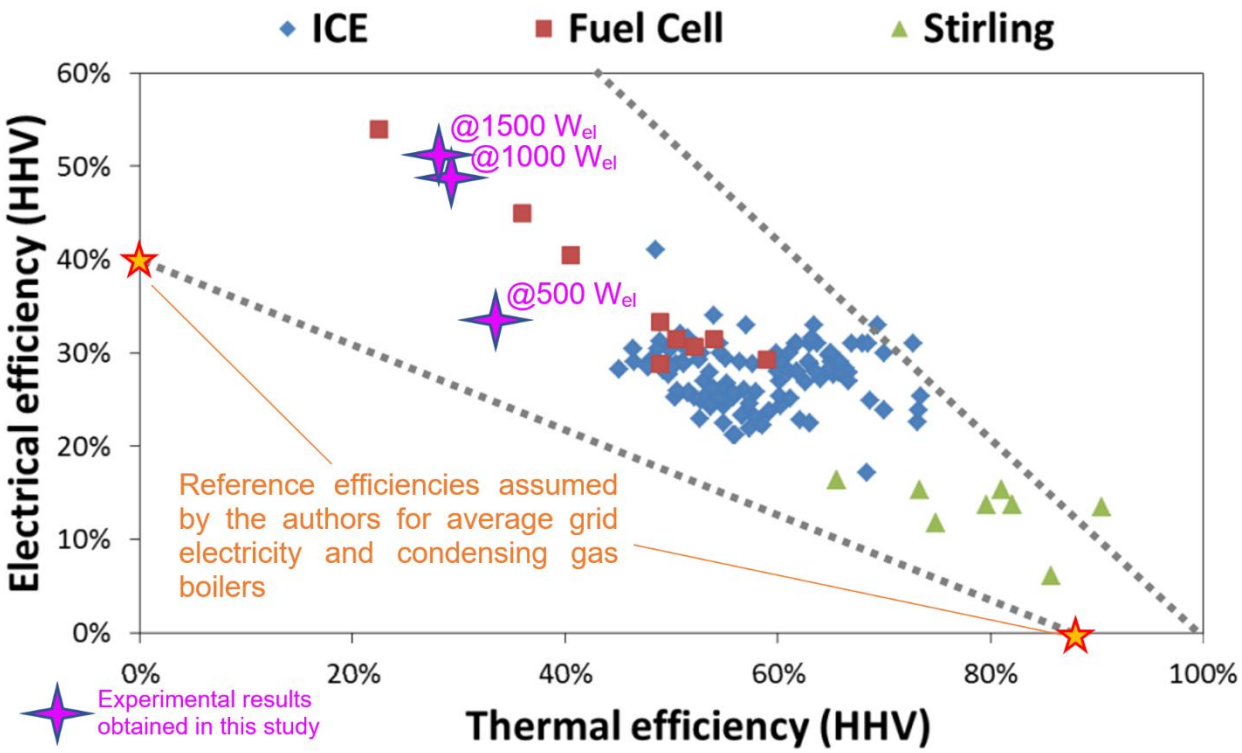

Figure 11. *Market study on reported efficiencies for three different groups of micro-CHPs: Internal Combustion Engines (ICE), Fuel Cell based micro-CHPs and CHP based on Stirling principle. Reproduced and adapted from reference [27].*

5.3. *Water consumption (and evacuation)*

As explained in the field-test study previously published about that particular SOFC [9], the system consumes water (discontinuously, a few times a day) from the mains in order to (filter and) store water that could later on help provide steam for methane reforming purposes. Even though a water meter was placed on the test bench (at the water mains connection), in such steady-state tests, the water consumption can hardly be related to the operating conditions as water withdrawals are only executed periodically (a few times a day). Indeed, generally, no water consumption was observable while conducting the test procedure for one particular set of operating conditions. For example, water withdrawal occurred a couple hours later, while the test campaign was finished or while conducting the test for other operating conditions.

However, from 20th September 2021 to 16th February 2022, the SOFC was turned on in the laboratory facilities and has provided (continuously, mostly at its nominal power output) 5048 kWh_{el} of electrical energy and 1434 kWh_{th} of heat. During that time, the system consumed 6274 L of water from the grid. This accounts for a water consumption of 1.24 L/kWh_{el}. This figure can be considered as in the upper range related to this SOFC system because, in the laboratory facilities, the heat recovery circuit was turned off most of the time (except during the three days of the actual test campaigns). Therefore, the return temperature was generally not cooled down and water in the flue gases was less likely to condensate and be fed back to the internal tank, which would have reduced the water consumption from the mains [9].

As shown in Figure 2, the system has two water outlets to the sewers (that have not been instrumented as water evacuations are quite sporadic). The first outlet evacuates brine water from a reverse osmosis filter [33] that cleans the water supply (from the mains) and feeds an internal tank (with cleaned water required for steam reforming processes of the inlet fuel, that is subsequently processed by the fuel cell stack) [9]. With such a two-chamber filter (separated with a filtering membrane), the water impurities concentration in the periodical inlet water volume becomes too high compared to the pressure used for the reverse osmosis. Thus, the remaining inlet water (with high levels of impurities) has to be thrown

away for another periodical grid fresh water inlet to take place (and to be submitted to the reverse osmosis filter). The more water is consumed from the grid, the more brine water will be evacuated.

As mentioned here above, flue gases are ideally cooled down by the optional heat recovery circuit and the condensates, which are not required to be processed in the reverse osmosis filter, are recovered and fed to the internal water tank [9]. However, this latter might be full so a second water outlet to evacuate its potential excess has been implemented [9].

Thus, enabling the heat recovery circuit and allowing for more processed water recovery (from the flue gases) will increase the probability of water excess in the internal tank (and water evacuation from the second outlet), but it will more importantly reduce water consumption from the grid and the resulting brine water evacuation (from the first outlet).

6. Conclusion

Electrical and thermal performance (efficiencies) models of the studied SOFC mCHP system are demonstrating great goodness of fit. Its electrical power output is tremendously stable and corresponds quite accurately to the output power setting as well as to the performance announced by the manufacturer (especially considering ageing). Along with the stable gas consumption, this leads to very stable electrical efficiencies. The electrical efficiency (and power output) is not altered at all by changes in working temperature of the heat recovery circuit (nor by potential change in heat recovery flow rate). In the tested range (corresponding to the range of a variable speed regular space heating circulator), thermal efficiency is almost not altered by the heat recovery flow rate.

Thermal efficiency is affected by the working temperature of the heat recovery circuit quite linearly and it decreases as working temperature increases. The slope of that linear decrease increases exponentially as electrical power output decreases. Indeed, at nominal electrical power output (1500 W), the thermal efficiency increase between about 50°C and 20°C of return temperature is about 26 percentage points. And, over a similar temperature range at minimal electrical output power (500 W), the thermal efficiency decrease reaches 35 percentage points. At nominal electrical power output (1500 W), highest LHV thermal efficiency is about 42% whereas it increases up to about 55% at minimal electrical power output (500 W).

The efficiency results at 1000 W of electrical power output are really close to the one obtained at 1500 W of electrical power output (for both electrical and total efficiency). However, lowering the electrical power output down to 500 W mainly reduces the electrical efficiency, which is not balanced by the increase of the thermal efficiency, meaning that the total efficiency still decreases compared to higher power output settings. Total LHV efficiency is indeed about 78% at 500 W of electrical power output whereas it comes close to 90 % at 1000 W and 1500 W of electrical power output.

The LHV thermal efficiency of 25% at nominal electrical output power of 1500 W announced by the manufacturer seems to correspond to a return of 40°C, which is relevant for many residential DHW applications. This corresponds to about 600 W of heat recovered. Residential DHW represents thus a suitable way of recovering the heat provided with the system. As explained, lowering the return temperature (without significantly reduce the heat recovery flow rate below the operating range of the variable speed circulator that has been used) would even increase the amount of heat recovered (and the thermal efficiency of the system) but at temperature lower than 40°C, it would no longer be convenient for DHW production.

Compared with CHP literature, this SOFC technology demonstrates quite high electrical efficiencies and satisfactory thermal efficiencies. In fact, no commercialized CHP system exhibiting higher electrical efficiencies than this system have been found by the authors of this paper.

Bibliography

[1] Paulus N. Confronting Nationally Determined Contributions (NDCs) to IPPC's +2°C carbon budgets through the analyses of France and Wallonia climate policies. Journal of Ecological Engineering 2023;24. https://doi.org/10.12911/22998993/162984.

[2] Paulus N. Developing individual carbon footprint reduction pathways from carbon budgets: Examples with Wallonia and France. Renewable and Sustainable Energy Reviews 2024;198:114428. https://doi.org/10.1016/j.rser.2024.114428.

[3] Minh NQ, Shirley Meng Y. Future energy, fuel cells, and solid-oxide fuel-cell technology. MRS Bull 2019;44:682–3. https://doi.org/10.1557/mrs.2019.209.

[4] Paulus N, Lemort V. Grid-impact factors of field-tested residential Proton Exchange Membrane Fuel Cell systems. Proceedings of the 14th REHVA HVAC World Congress (CLIMA2022) 2022. https://doi.org/10.34641/CLIMA.2022.176.

[5] Paulus N, Dávila C, Lemort V. Field-test economic and ecological performance of Proton Exchange Membrane Fuel Cells (PEMFC) used in micro-combined heat and power residential applications (micro-CHP). Proceedings of the 35th International Conference On Efficiency, Cost, Optimization, Simulation and Environmental Impact of Energy Systems (ECOS2022) 2022. https://doi.org/10.11581/dtu.00000267.

[6] Paulus N. Decarbonization potentials of fuel cell technologies in micro-cogeneration application. Progress in Energy 2024; In Press.

[7] Paulus N, Lemort V. Pollutant testing (NOx, SO2 and CO) of commercialized micro-combined heat and power (mCHP) fuel cells. Proceedings of the 36th International Conference On Efficiency, Cost, Optimization, Simulation and Environmental Impact of Energy Systems (ECOS2023) 2023. https://doi.org/10.52202/069564-0104.

[8] Paulus N, Lemort V. Experimental assessment of pollutant emissions from residential fuel cells and comparative benchmark analysis. J Environ Manage 2024;359:121017. https://doi.org/10.1016/j.jenvman.2024.121017.

[9] Paulus N, Lemort V. Field-test performance of Solid Oxide Fuel Cells (SOFC) for residential cogeneration applications. Proceedings of the 7th International High Performance Buildings Conference at Purdue (Herrick 2022) 2022.

[10] Dikwal CM, Bujalski W, Kendall K. The effect of temperature gradients on thermal cycling and isothermal ageing of micro-tubular solid oxide fuel cells. J Power Sources 2009;193:241–8. https://doi.org/10.1016/j.jpowsour.2009.01.097.

[11] Nakajo A, Mueller F, Brouwer J, Van herle J, Favrat D. Mechanical reliability and durability of SOFC stacks. Part II: Modelling of mechanical failures during ageing and cycling. Int J Hydrogen Energy 2012;37:9269–86. https://doi.org/10.1016/j.ijhydene.2012.03.023.

[12] Paulus N, Lemort V. Experimental investigation of a Solid Oxide Fuel Cell (SOFC) used in residential cogeneration applications. Proceedings of the 36th International Conference On Efficiency, Cost, Optimization, Simulation and Environmental Impact of Energy Systems (ECOS2023) 2023. https://doi.org/10.52202/069564-0056.

[13] Paulus N. Comprehensive assessment of fuel cell types: A novel fuel cell classification system. Submitted in International Journal of Hydrogen Energy 2024. https://doi.org/10.2139/ssrn.4800979.

[14] Aguiar P, Chadwick D, Kershenbaum L. Effect of methane slippage on an indirect internal reforming solid oxide fuel cell. Chem Eng Sci 2004;59:87–97. https://doi.org/10.1016/j.ces.2003.09.022.

[15] Paulus N, Job N, Lemort V. Investigation of degradation mechanisms and corresponding recovery procedures of a field-tested residential cogeneration Polymer Electrolyte Membrane fuel cell. To Be Submitted 2024.

[16] Paulus N, Lemort V. Simplified test bench for experimental investigations of space heating appliances. IOP Conf Ser Earth Environ Sci 2023;1185:012014. https://doi.org/10.1088/1755-1315/1185/1/012014.

[17] European Commission. EN 13757-4 - Communication systems for meters and remote reading of meters - Part 4: Wireless meter readout (Radio meter reading for operation in SRD bands). 2013.

[18] International Organization of Legal Metrology. OIML R 75-1: 2002 (E): Heat meters Part 1: General requirements Compteurs d'énergie thermique Partie 1: Exigences générales. 2002.

[19] Tegeler E, Heyer D, Siebert BerndRL. Uncertainty of the Calibration of Paired Temperature Sensors for Heat Meters. Int J Thermophys 2008;29:1174–83. https://doi.org/10.1007/s10765-008-0416-y.

[20] International Electrotechnical Commission. IEC 60751 : Industrial platinum resistance thermometers and platinum temperature sensors. 2022.

[21] Lombardi K, Ugursal VI, Beausoleil-Morrison I. Proposed improvements to a model for characterizing the electrical and thermal energy performance of Stirling engine micro-cogeneration devices based upon experimental observations. Appl Energy 2010;87:3271–82. https://doi.org/10.1016/j.apenergy.2010.04.017.

[22] International Electrotechnical Commission. IEC 62053-21: Electricity metering equipment (a.c.) – Particular requirements. Part 21 : Static meters for active energy (classes 1 and 2). 2003.

[23] Paulus N, Dávila C, Lemort V. Correlation between field-test and laboratory results for a Proton Exchange Membrane Fuel Cell (PEMFC) used as a residential cogeneration system. Proceeding of the 30th "Congrès Annuel de La Société Française de Thermique" (SFT 2022) 2022. https://doi.org/10.25855/SFT2022-119.

[24] Paulus N, Lemort V. Establishing the energy content of natural gas residential consumption : example with Belgian field-test applications. IOP Conf Ser Earth Environ Sci 2023;1185:012013. https://doi.org/10.1088/1755-1315/1185/1/012013.

[25] Föger Australia Other K, Rowe T. Ceramic Fuel Cells LTD Residential Generator BlueGen - Ultra-efficient distributed power generation in Smart Grid Environment. Proceedings of the 2nd International Gas Union Research Conference (IGRC 2011) 2011.

[26] Liso V, Olesen AC, Nielsen MP, Kær SK. Performance comparison between partial oxidation and methane steam reforming processes for solid oxide fuel cell (SOFC) micro combined heat and power (CHP) system. Energy 2011;36:4216–26. https://doi.org/10.1016/j.energy.2011.04.022.

[27] Verhaert I, Van Riet F, Baetens R, De Pauw M, Van Erdeweghe M. Performance evaluation of different micro-CHP configurations in real life conditions and the influence of part load behaviour. E3S Web of Conferences 2019;111:01084. https://doi.org/10.1051/e3sconf/201911101084.

[28] Paulus N, Lemort V. Field-test performance models of a residential micro-cogeneration system based on the hybridization of a proton exchange membrane fuel cell and a gas condensing boiler. Energy Convers Manag 2023;295. https://doi.org/10.1016/j.enconman.2023.117634.

[29] Payne R, Love J, Kah M. Generating Electricity at 60% Electrical Efficiency from 1 - 2 kWe SOFC Products. ECS Trans 2009;25:231–9. https://doi.org/10.1149/1.3205530.

[30] Staffell I. Zero carbon infinite COP heat from fuel cell CHP. Appl Energy 2015;147:373–85. https://doi.org/10.1016/j.apenergy.2015.02.089.

[31] Staffell I, Baker P, Barton JP, Bergman N, Blanchard R, Brandon NP, et al. UK microgeneration. Part II: technology overviews. Proceedings of the Institution of Civil Engineers - Energy 2010;163:143–65. https://doi.org/10.1680/ener.2010.163.4.143.

[32] CWaPE. Décision CD-5j18-CWaPE relative à "la définition des rendements annuels d'exploitation des installations modernes de référence, ..." 2005.

[33] Fritzmann C, Löwenberg J, Wintgens T, Melin T. State-of-the-art of reverse osmosis desalination. Desalination 2007;216:1–76. https://doi.org/10.1016/j.desal.2006.12.009.

